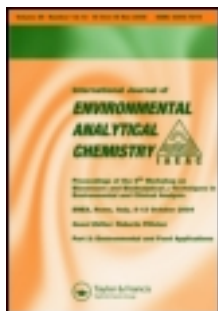


This article was downloaded by: [John Lambrinos]

On: 19 October 2011, At: 18:01

Publisher: Taylor & Francis

Informa Ltd Registered in England and Wales Registered Number: 1072954 Registered office: Mortimer House, 37-41 Mortimer Street, London W1T 3JH, UK



International Journal of Environmental Analytical Chemistry

Publication details, including instructions for authors and subscription information:

<http://www.tandfonline.com/loi/geac20>

Scaling confounds the interpretation of isotopic data

Timothy L. Righetti^a, Dan Dalthorp^b, John Lambrinos^c,
Bernadine Strik^c, David Sandrock^d & Claire Phillips^e

^a Division of National Sciences, University of Guam, Mangilao, GU, 96923, USA

^b Department of Statistics, Oregon State University, Corvallis, OR, 97331, USA

^c Department of Horticulture, Oregon State University, Corvallis, OR, 97331, USA

^d Portland Community College, Portland, OR, 97229, USA

^e Terrestrial Ecosystems Research Associates, 200 SW 35th St., Corvallis, OR 97333, USA

Available online: 12 Oct 2011

To cite this article: Timothy L. Righetti, Dan Dalthorp, John Lambrinos, Bernadine Strik, David Sandrock & Claire Phillips (2011): Scaling confounds the interpretation of isotopic data, International Journal of Environmental Analytical Chemistry, DOI:10.1080/03067319.2010.522236

To link to this article: <http://dx.doi.org/10.1080/03067319.2010.522236>



PLEASE SCROLL DOWN FOR ARTICLE

Full terms and conditions of use: <http://www.tandfonline.com/page/terms-and-conditions>

This article may be used for research, teaching, and private study purposes. Any substantial or systematic reproduction, redistribution, reselling, loan, sub-licensing, systematic supply, or distribution in any form to anyone is expressly forbidden.

The publisher does not give any warranty express or implied or make any representation that the contents will be complete or accurate or up to date. The accuracy of any instructions, formulae, and drug doses should be independently verified with primary

sources. The publisher shall not be liable for any loss, actions, claims, proceedings, demand, or costs or damages whatsoever or howsoever caused arising directly or indirectly in connection with or arising out of the use of this material.

Scaling confounds the interpretation of isotopic data

Timothy L. Righetti^{a*}, Dan Dalthorp^b, John Lambrinos^c,
Bernadine Strik^c, David Sandrock^d and Claire Phillips^e

^aDivision of National Sciences, University of Guam, Mangilao, GU, 96923, USA;

^bDepartment of Statistics, Oregon State University, Corvallis, OR, 97331, USA;

^cDepartment of Horticulture, Oregon State University, Corvallis, OR, 97331, USA;

^dPortland Community College, Portland, OR, 97229, USA; ^eTerrestrial Ecosystems
Research Associates, 200 SW 35th St., Corvallis, OR 97333, USA

(Received 2 July 2009; final version received 2 September 2010)

We demonstrate that delta values (δ) and other relative ratio-based isotopic expressions can vary with the total amount of isotopes present in the system or subject being evaluated. Although these scaling effects are routinely overlooked, interpretive errors such as noting of spurious treatment effects or not detecting significant effects may occur. Algebraic conversions of linear or log-log equations (rare isotope predicted by common or total isotope) that suggest apparently miniscule scaling will fit the observed relationship between isotopic ratios and total or common isotopes. When the ranges of scaling induced differences in isotopic ratios are converted to the equivalent discrimination expressions (Δ) or delta values (δ), differences are within the range that is generally reported in the isotopic literature. Therefore, interpreting observed differences in isotopic ratios may require an evaluation to determine whether treatments directly affect how a rare isotope is accumulated or are associated with differences in denominator size. If effects are direct, points for different treatments fall on different linear and log-log (total isotope vs. rare isotope or common isotope vs. rare isotope) regression lines. Slope differences or derivatives may be more revealing than changes in isotopic ratios and better represent system change in a scaling system. By simply recording total common isotope or total elemental content, standard statistical procedures that evaluate changes in slopes or derivatives can be combined with an ANCOVA to better evaluate isotopic data. In many cases, scaling issues will not interfere with interpretations. In other situations it may be difficult to untangle a combination of ubiquitous scaling, treatment induced scaling and direct treatment effects.

Keywords: carbon isotopes; delta values; nitrogen isotopes; ratios; regression; slope-based assessments

1. Introduction

Isometric scaling (or no scaling) can be defined as the condition where a ratio Y/M does not depend on denominator size. If the value of a ratio depends on its denominator, allometric scaling occurs. The terminology attributed to allometric scaling was first coined in 1936 [1]. Since then scaling relationships have been extensively studied [2–4] and are often modelled as a power law $Y = Y_0M^b$, where Y is some physiological, morphological,

*Corresponding author. Email: trighetti@ugam.uog.edu

or ecological characteristic that varies with another characteristic M (typically body mass). In our isotopic application Y represents a rare isotope and M represents total or common isotope. Hereafter, total isotope refers to total elemental content.

Log Y vs. log M plots produce a slope equal to the scaling exponent. Allometric scaling (or simply *scaling*) occurs when $b \neq 1$, and the ratio Y/M is then dependent on denominator size. A ratio is also dependent on its denominator (scaling occurs) if the relationship between denominator and numerator is described by a linear function with a non-zero y -intercept [5–8]. In a scaling system where individuals have different amounts of total M (total or common isotope) the ratio Y/M (rare isotope : common isotope or rare isotope : total isotope) in sampled individuals will be statistically related to M . Since total isotope and common isotope are almost always strongly correlated to organism size, isotopic ratios are often dependent on the sizes of the organisms or other subject pools being studied.

Studies where ratios lead to biased or even opposite conclusions than what a direct evaluation of the relationship between numerators and denominators reveal are well documented [5,8–14]. Packard and Boardman [11] suggested that researchers avoid using ratios and use an analysis of covariance (ANCOVA) instead. Raubenheimer and Simpson [15] make a similar argument. Every use of ratios must be based on knowledge of ratio behaviour in respect to size changes [8–10,13].

Since ratios can scale with size (whatever size is; body mass, total amount of isotopes etc.), their use has been widely abandoned in many comparative studies; especially in morphometrics [8]. It is thus surprising that ratio-based expressions are widely used in isotopic studies without any testing of the isometric assumption that justifies their use. If the isometric assumption is not met, ratio-based expressions are an inappropriate attempt to correct for differences in total isotope. Ecologists often study how ratio-based isotopic expressions change with time, treatment or trophic level. However, in many cases total isotope content is not measured or rigorously evaluated.

One could argue that correcting for size differences is sometimes inappropriate. For example, larger fish eating bigger and more enriched ^{15}N prey are expected to have more enriched $^{15}\text{N} : ^{14}\text{N}$ composition. Statistically removing the size-effect does not change the fact that larger fish are indeed more enriched. However, one may want to determine whether or not two species fundamentally differ in isotopic composition independent of expected differences due to size alone. Perhaps a very large individual from a small species is similar in its rare isotope accumulation to a small individual from large species. Similar sized individuals from different species may not differ. Alternatively a small species with a lower $\delta^{15}\text{N}$ value than a large species may physiologically or behaviourally differ and accumulate similar, more or less ^{15}N on an equal size basis. Without replicate total common and rare isotope data, it is impossible to untangle inherent species differences and associated size effects. We advocate routine evaluations for both direct and indirect (total isotope related) effects.

At first glance, it may appear that there is no a priori reason to suspect that ratio-based isotopic expressions necessarily scale with total isotope in a natural system. However, there are fundamental conceptual reasons to hypothesise that isotopic ratios scale. Detailed conceptual examples are included in a supplementary document [16]. A brief discussion of several possible mechanisms is described below.

One possible explanation for allometric scaling is that metabolic rates decline with increasing animal size [2–4]. This suggests that turnover and changes in isotopic ratio could also scale with body size. Isotopic ratios in smaller organisms could more quickly

approach the more enriched or depleted isotopic composition of a new food source because they have higher metabolism rates and faster isotopic turnover. Although this mechanism is based on temporal differences that would disappear at equilibrium, many ecological systems are constantly perturbed and never reach a stable state.

An isometric system where the plot of total common {*x*-axis} vs. total rare isotope {*y*-axis} is linear with a zero *y*-intercept as common isotope accumulates is to be expected as organisms grow when exposed to a food source with constant isotopic composition. However, an interruption of an established isometric system with a different rate of rare isotope accumulation as common isotope increases will result in a scaling system [7,16]. A new uptake trajectory must produce functions with a different slope and a non-zero *y*-intercept, even if the new accumulation relationship remains linear.

In cyclic systems a total common isotope {*x*-axis} vs. total rare isotope {*y*-axis}, loss trajectory that differs from an isotope accumulation curve will also cause scaling. Even if isotopic uptake relationships remain unchanged during a second accumulation cycle, a new trajectory cannot remain isometric (linear with a zero *y*-intercept). It is not realistic to expect cyclic systems to always gain and lose rare isotopes along the same isometric line as total or common isotopes increase or decline. Therefore, any system with consistent hysteresis can produce allometric scaling over time, even if the hysteresis effect is quite small for a single cycle. Perturbation and hysteresis effects likely confound true metabolism-based biological scaling relationships, producing complex isotopic scaling relationships that are difficult to predict or explain without a thorough understanding of system history. Scaling effects may also arise from experimental variation and measurement error [14].

Studies examining stable isotopes at or near natural abundance levels are usually reported as delta values (δ) in parts per thousand or per mil (‰). Delta values and other isotopic conventions describe relative differences between samples and a standard. Therefore, common isotopic expressions are not absolute isotope abundances but differences between sample readings and one or another of the widely used natural abundance standards routinely used in isotopic research. For example $\delta^{15}\text{N}$ values are defined as:

$$\delta^{15}\text{N} \text{ ‰ vs. [std]} = [(R_{\text{sample}} - R_{\text{std}})/R_{\text{std}}] * 1000$$

or

$$\delta^{15}\text{N} \text{ ‰ vs. [std]} = [(R_{\text{sample}}/R_{\text{std}}) - 1] * 1000$$

where absolute isotope ratios (*R*) are measured for sample and standard.

The value *R* is a ratio based on absolute numbers (At%) of atoms of a given isotope in 100 atoms of total element. In this case:

$$R = \text{At } \%^{15}\text{N} / \text{At } \%^{14}\text{N}$$

Delta values defined as above and other relative isotopic expressions can be algebraically converted to an isotopic ratio (rare isotope to common or total isotope). However, making this conversion requires precise knowledge of the absolute ratio in the scale-defining ratio, which is non-trivial. Delta values are used not only because they make for more convenient numbers to discuss, but also because they allow researchers to evaluate deviations from a standard with an imperfectly-known actual isotopic ratio.

In spite of the many good reasons for using relative isotopic expressions, they are subject to the same mathematical principles and statistical limitations that apply to any ratio. Therefore, we argue that routinely measuring total elemental content in individual subjects (not the elemental content of the sample) is important. In the analyses that follow, original data that were reported as either δ or Δ values were converted to rare isotope : common isotope or rare isotope : total isotope ratios. The total, common and rare isotope content for individual subjects were then calculated for statistical evaluation.

Scaling effects can alter interpretations in tracer studies [6,7]. Published accounts also suggest that metabolic-based scaling can complicate the interpretation of natural abundance isotopic ratios. Carelton and del Rio [17] present data showing the rate of ^{13}C incorporation into birds scales with bird size. In Jennings *et al.* [18], isotopic ratios are also dependent on organism size. In del Rio *et al.* [19], the authors discuss the need to consider body size when comparing isotopic composition among species. We want to reiterate this important concept while emphasising that even apparently miniscule scaling, if unaccounted for, can alter interpretation.

Log-log slopes that differ from 1 only by incredibly small margins (for example ± 0.001 or smaller) can still be mathematically and statistically important. Very small non-zero y -intercepts for linear functions are also important. Algebraic conversions of linear or log-log equations that suggest apparently miniscule scaling will fit the observed relationship between isotopic ratios and total or common isotopes. If these relationships did not statistically scale (for example, scaling exponents equal 1.000; rather than 0.999 or 1.001), there would not be a statistically significant relationship between an isotopic ratio and its denominator. The range in isotopic ratios that are commonly evaluated in ecological and environmental studies is so small that even miniscule scaling effects influence interpretation. If an isometric assumption is not met, using ratios to compensate for size-related total isotope differences is inappropriate, regardless of the source of observed scaling.

It is not intuitively obvious whether a slope (change in rare isotope relative to the change in common isotope) increases or decreases when only δ values are evaluated. Therefore, we also advocate the use of derivatives in addition to conventional ratio-based δ values. A derivative reflects the incremental gain or loss in rare isotope as total or common isotope changes and reflects the isotopic composition of the element removed or added to the system. In the often-used Keeling plot [20], $1/\text{total CO}_2$ concentration (x -axis) is plotted against $\delta^{13}\text{C}$ (y -axis). The y -intercept of the least squares line is commonly assumed to be the δ -value of the CO_2 source. A similar plot of $1/\text{total CO}_2$ (x -axis) vs. $^{13}\text{CO}_2$: total CO_2 ratio (y -axis) could be constructed where the y -intercept represents the ^{13}C : total CO_2 ratio of the CO_2 source. The $^{13}\text{CO}_2$: $^{12}\text{CO}_2$ source ratio could be similarly obtained by determining the y -intercept of a $1/\text{total } ^{12}\text{CO}_2$ vs. $^{13}\text{CO}_2$: $^{12}\text{CO}_2$ plot.

Mathematically, the y -intercept b of the curve $y/x = a/x + b$ is simply the slope of the line $y = a + bx$. Thus, the inverse total CO_2 vs. $^{13}\text{CO}_2$: total CO_2 plot is simply an indirect way of approximating the slope of the linear relationship between total CO_2 (x -axis) plotted against $^{13}\text{CO}_2$ (y -axis). We suggest that directly calculating a derivative ($d^{13}\text{CO}_2/d$ total CO_2 or $d^{13}\text{CO}_2/d^{12}\text{CO}_2$) and observing how it changes as total isotope increases or declines is a more appropriate way to assess composition changes than indirectly calculating the slope of a linear function when the original data may not be linear.

The following experimental examples support the theoretical scaling effects presented above. Different-sized denominators (that reflect different total elemental content in individual subjects) cause interpretive difficulties. We emphasise that when total isotope content is known, three important evaluations can be made: (1) one can determine whether

or not a ratio-based statistical model that assumes isometric scaling is appropriate, (2) the derivative (d rare isotope/d total isotope or d rare isotope/d common isotope) can be calculated, and (3) the data can be evaluated to determine if indirect scaling effects alter isotopic ratio interpretation. The fact that total rare or common isotope analyses are both analytically challenging and logistically cumbersome, does not justify routine statistical evaluations of ratio-based expressions without testing the isometric assumption that justifies their use.

2. Experimental

Measurements of $\delta^{13}\text{C}$, $\Delta^{13}\text{C}$, $\delta^{15}\text{N}$ or $^{15}\text{N}:^{14}\text{N}$ ratio were collected from the following published studies: (1) Righetti *et al.* [6]: ^{15}N tracer studies for shoot and root tissues in N fertilised ornamental shrubs; (2) Minagawa and Wada [21]: evaluations of $\delta^{15}\text{N}$ in both a relatively small mussel species (*Septifer virgatus*) and a relatively large mussel species (*Mytilus edulis*); (3) Hubick *et al.* [22] and Condon *et al.* [23]: relationships between dry weight and $\Delta^{13}\text{C}$ in peanut (*Arachis hypogaeae*) and wheat (*Triticum aestivum*); (4) Rau *et al.* [24]: relationships between $^{15}\text{N}:^{14}\text{N}$ ratio and fresh weight for Dover sole (*Microstomus pacificus*) grown in polluted and unpolluted costal sites; (5) Jennings *et al.* [18]: an evaluation of $\delta^{15}\text{N}$ for three (zooplankton, small fish, large fish) of the five faunal groups the authors originally evaluated; (6) Keeling *et al.* [25] and Keeling *et al.* [26]: global carbon studies on the seasonal oscillation in $\delta^{13}\text{C}$ values that are observed in the Northern hemisphere; and (6) Francey *et al.* [27] and Friedli *et al.* [28]: global carbon studies on the decline in atmospheric $\delta^{13}\text{C}$ over time derived from Antarctic ice core and firn samples.

Measurements of total C or total N were evaluated when available. When total C or total N were not available, they were estimated from literature values of the C and N concentrations of the species involved. For the global carbon evaluations, total CO_2 concentration in the atmosphere was used as a proxy for total C. We assume that rising or falling CO_2 amounts in a constant volume reflect total CO_2 changes. All values for $\delta^{13}\text{C}$ or $\delta^{15}\text{N}$ were converted to the respective isotopic $^{13}\text{C}:\text{total C}$, $^{13}\text{C}:^{12}\text{C}$, $^{15}\text{N}:\text{total N}$, $^{15}\text{N}:^{14}\text{N}$, $^{13}\text{CO}_2:\text{total CO}_2$, or $^{13}\text{CO}_2:^{12}\text{CO}_2$ ratios. We then used these ratios to calculate the ^{13}C , ^{15}N or $^{13}\text{CO}_2$ values that would be associated with the measured or estimated total C, total N and total CO_2 or ^{12}C , ^{14}N or $^{12}\text{CO}_2$.

Plots of ^{12}C (or total C) vs. ^{13}C , ^{14}N (or total N) vs. ^{15}N and $^{12}\text{CO}_2$ (or total CO_2) vs. $^{13}\text{CO}_2$ were then evaluated to determine if relationships statistically scale using SYSTAT software (TableCurve[®] 2D, version 5.01; San Jose, Calif.). Log-log versions of the same relationships were also statistically evaluated. The choice of defining the M term with either common isotope or total isotope (for example ^{13}C vs. ^{12}C or $(^{12}\text{C} + ^{13}\text{C})$) can alter scaling evaluations since mathematical relationships are not the same. However, in our examples, statistical conclusions did not change when either approach was used. None-the-less we have chosen to present the simpler unconfounded common isotope vs. rare isotope analyses in all but the global carbon example.

MiniTab (version 15; Minitab Inc, State College, Pennsylvania) and SAS statistical software (version 9.1; SAS Institute, Cary, N.C.) were used to conduct an analysis of Covariance (ANCOVA) where either isotopic ratios, rare isotope or \log_{10} rare isotope were analyzed with the inverse of total isotope, total isotope or \log_{10} total isotope as the

respective covariates to evaluate whether significant treatment effects for isotopic ratios could be attributed to scaling effects.

Scaling exponents where $b \neq 1$ imply that ratios are dependent on their denominators. However, the fact that a log-log plot with a slope not equal to 1.0 fits a data set does not necessarily imply statistical curvature in the untransformed data. Linear functions with non-zero y -intercepts can be very well approximated with curvilinear power functions that implicitly assume zero y -intercepts. Therefore, SYSTAT TableCurve[®] 2D software was used to evaluate curvature in the original non-transformed relationships described above by evaluating the statistical significance of the x^2 term in polynomial ($y = ax + bx^2 + c$) best-fit equations. Curvature was also evaluated by evaluating intercept inclusive power functions ($y = c + ax^b$) for b not equal to 1.0 and statistical significance in a . Since a combination of linear functions with no statistical curvature that describe individual treatments can produce significant polynomial fits when all data points are analyzed, curvature was evaluated for both individual treatments and combined data sets. Since both polynomial and intercept inclusive power function approaches for curvature detection, when statistically significant, generally support similar conclusions, and since polynomial fits usually had higher r^2 values, only p values for polynomial significance are presented unless the power function better explained the data.

Statistically significant curvature was also described by calculating derivatives (either d rare isotope/ d total isotope or d rare isotope/ d common isotope) for either the total isotope vs. rare isotope or common isotope vs. rare isotope relationships. Cubic functions with 7 knots were used to calculate the spline smoothed derivatives in SYSTAT software.

3. Results and discussion

We discuss confounding scaling effects that if overlooked, lead to misleading conclusions. In the first example, scaling effects both created a spurious difference among plant species and masked a significant difference between tissues in a ^{15}N tracer study [6]. In the second example, scaling obscures real differences among species in a study of invertebrate stable N isotope composition [21]. In the third example we demonstrate that scaling occurs in the accumulation of ^{13}C relative to ^{12}C in plants grown with adequate moisture [22,23]. A fourth example indicates how both treatments (polluted and unpolluted food sources) and scaling can affect isotopic N ratios in fish [24]. In the fifth example, we consider a case where body size varied across size fractionated classes spanning six orders of magnitude, thus a confounding of scaling and trophic effects is observed [18]. A global carbon example is used to demonstrate how changing conditions can induce scaling effects that complicate other ongoing analyses [25–28].

3.1 Scaling occurs in the accumulation of ^{15}N relative to ^{14}N in a tracer study

Righetti *et al.* [6] have demonstrated that the amount of N in plants that is derived from fertiliser can scale with total N uptake. A portion of their data is presented to demonstrate the statistical and mathematical properties that can confound isotopic ratios. In this and all subsequent examples, interpretation of the differences in ratio-based isotopic expressions among different-sized samples may be more complex than what is traditionally assumed. A tracer study was selected as our first example because differences are clearly apparent in either the untransformed or log-log plots presented in Figure 1. Although the

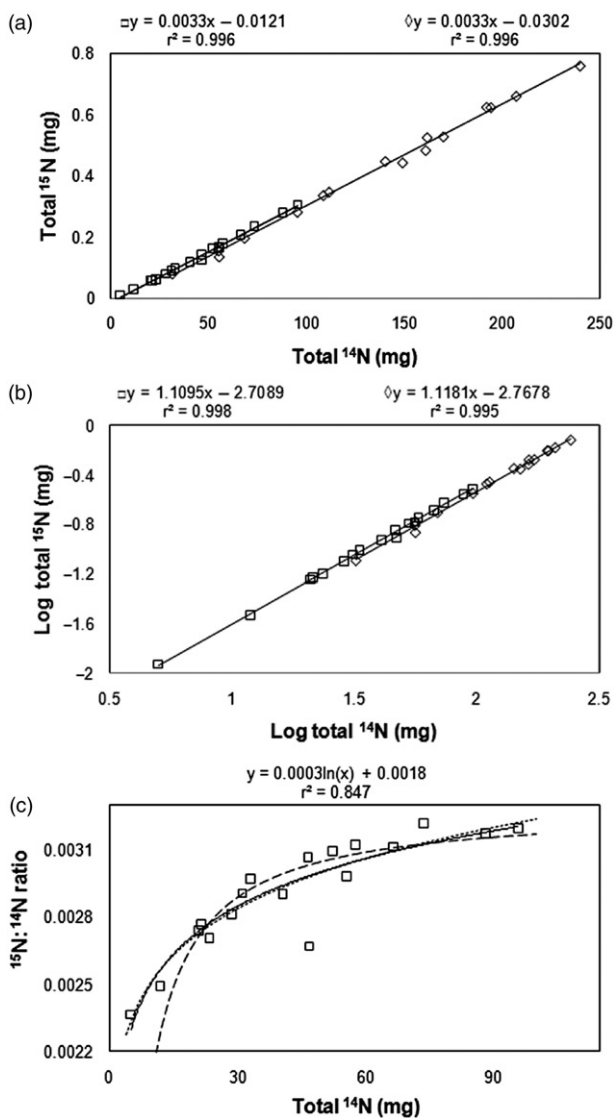


Figure 1. Scaling relationships for ^{15}N with ^{14}N . (a) Total ^{14}N vs. total ^{15}N for root (\diamond) and shoot (\square) tissues from three ornamental shrub genera (*Weigela*, *Cornus* and *Euonymus* grown at $25 \mu\text{g g}^{-1}$ of applied N in a tracer study that utilised depleted ^{15}N). (b) $\text{Log}_{10} ^{14}\text{N}$ vs. $\text{log}_{10} ^{15}\text{N}$ for the same ornamental shrub genera data presented in a. (c) ^{14}N vs. $^{15}\text{N}:^{14}\text{N}$ ratio of shoot tissue for the same ornamental shrub genera data presented in a. The predicted relationships implied by the untransformed linear function (---) in a, the log-log transformed power function (—) in b, and a logarithmic best fit equation (—) are all shown. Data derived from Righetti *et al.* [6].

same principles apply, more subtle, and often visually undetectable but still significant, differences in the natural abundance examples that follow are not as easy to conceptually visualise. In natural abundance studies linear relationships with miniscule non-zero intercepts or log-log scaling exponents that only slightly differ from 1.0 have scaling implications.

Table 1. Differences among ornamental shrubs (*Cornus sericea*, *Euonymus altus* and *Weigela florida*) and root and shoot tissues for least square means of $^{15}\text{N}:^{14}\text{N}$ ratio, covariate adjusted total ^{15}N and covariate adjusted log total ^{15}N for plants grown under greenhouse conditions. Respective covariates for ^{15}N and log ^{15}N were ^{14}N and log ^{14}N . Plants were grown at $25\ \mu\text{g g}^{-1}$ of applied N in a tracer study that utilised depleted ^{15}N . Data derived from Righetti *et al.* [6].

	$^{15}\text{N}:^{14}\text{N}$ ratio	Covariate adjusted Total ^{15}N	Covariate adjusted log total ^{15}N
Species			
<i>C. sericea</i>	0.00306 a ^z	0.264 a	-0.729 a
<i>E. alatus</i>	0.00271 b	0.266 a	-0.731 a
<i>W. florida</i>	0.00309 a	0.255 a	-0.745 a
Plant tissue			
Root	0.00300 a	0.250 a	-0.760 a
Shoot	0.00291 a	0.274 b	-0.710 b

^zValues for species or plant tissue that are followed by the same letter are not significantly different ($p < 0.05$; Tukey multiple comparisons).

The $^{15}\text{N}:^{14}\text{N}$ ratio was evaluated in both root and shoot tissues in three species of ornamental shrubs [6]. Values for species and plant tissue main effects (tissue \times species interaction not significant, $p < 0.783$) are presented in Table 1. The smallest species has a statistically smaller $^{15}\text{N}:^{14}\text{N}$ ratio than the two larger species ($p < 0.0001$). The question we want to answer is if these species differences are indirectly due to size and total N uptake differences among the three species or related to fundamentally different fertiliser N uptake for the smaller species. Perhaps a very large *Euonymus* plant that was similar in size and N uptake to small *Cornus* or *Wygeilia* plants is physiologically similar with respect to rare isotope accumulation. If effects are indirect, replicates of all three species will fall on the same allometric regression line. If effects are direct, replicate points for individual species will fall on different regression lines. From a visual examination of the data in both the untransformed (Figure 1a) and log-log (Figure 1b) plots of total ^{14}N vs. total ^{15}N all points within a tissue type appear to fall on the same regression lines.

A statistical approach to verify that points for different species do indeed fall on the same allometric regression lines uses either ^{14}N or log ^{14}N as respective covariates in an ANCOVA conducted on ^{15}N or log₁₀ ^{15}N . Since there are no covariate \times species, covariate \times tissue type or covariate \times tissue type \times species interactions in our example, the ^{14}N vs. ^{15}N or log ^{14}N vs. log ^{15}N slopes are statistically similar and the three interaction terms can be dropped from the ANCOVA for either the untransformed or log-log models. An ANCOVA without interaction terms can then be used to determine if regression lines are similar or if intercepts differ. In our example, all species fall on the same regression line within a tissue, but shoots and roots although they have the same slope, fall on different allometric regression lines. The final ANCOVA can then be used to produce ^{15}N or log ^{15}N covariate adjusted mean values that account for differences in total ^{14}N shown in Table 1. ANCOVAs for both untransformed and log-log models where the highest order interaction (covariate \times tissue type \times species), followed by the most significant two-factor interaction term, and then the final two-factor interaction term were sequentially removed are presented in (Supplementary Statistical Details). All other

ANCOVA analyses that are described below were conducted in a similar manner. A standard ANOVA on the $^{15}\text{N}:^{14}\text{N}$ ratio is also included in this supplemental material.

We found significant ($p < 0.001$) species differences in the $^{15}\text{N}:^{14}\text{N}$ ratio (Table 1). There were no differences among tissues. The full-factorial GLM model determined that only the effects of total ^{14}N ($p < 0.001$) and tissue type ($p < 0.002$) were significant. Species and species \times tissue interactions were not significant. The intercepts (b) of the common allometric lines were significantly less than zero for both tissues ($p < 0.003$ for both tissues). The slope of the common log-log regression lines were again in both cases significantly greater than 1 ($p < 0.003$ for both tissues). Therefore, the $^{15}\text{N}:^{14}\text{N}$ ratio must necessarily increase with increasing total N as is shown for the shoot tissue in Figure 1c. The predicted relationships implied by the untransformed linear function in Figure 1a, the log-log transformed power function in Figure 1b, and a logarithmic best fit equation are all shown.

We can thus conclude that the trend for lower $^{15}\text{N}:^{14}\text{N}$ ratio in the smallest species is then an epiphenomenon of less total N uptake in comparison with the other species. Although tissue types appear to visually fall on different allometric regression lines in Figure 1a and b, no statistical differences in $^{15}\text{N}:^{14}\text{N}$ ratio for tissue type were detected in a standard ANOVA (Table 1). A scaling effect masked significant differences in tissue type that are only revealed when differences in total N are accounted for in an ANCOVA using either untransformed or log-log transformed data. Scaling effects both created a spurious difference among species and masked a significant difference between tissues. The x^2 term for a polynomial fit of the relationship between ^{15}N and ^{14}N was not statistically significant for either individual or combined species in either shoot or root tissues.

3.2 Scaling masks significant effect for the accumulation of ^{15}N relative to ^{14}N

The $\delta^{15}\text{N}$ values for a relatively small mussel species (*Septifer vigrutus*) and a relatively large species (*Mytilus edulis*), were not significantly different [21]. Over time, the $\delta^{15}\text{N}$ values initially increased then declined, approaching, but still greater than, the value of the food source for *S. vigrutus*. *Mytilus edulis* showed a similar initial increase, but the subsequent decline was less distinct [21]. We evaluated scaling in both species. Our goals were (1) to demonstrate that log-log slopes that differ from 1 only by incredibly small margins can still be mathematically and statistically important; and (2) to demonstrate how regression and ANCOVA could reveal significant differences in ^{15}N accumulation in the two species that are obscured if size related total N differences are not taken into account.

In this example, we use ^{14}N to approximate total N. Shell length in the original reference was related to total ^{14}N for both species (r^2 values of 0.95 and 0.97 for *S. vigrutus* and *M. edulis*, respectively), and the species with greater total N had longer shells. A plot of $\log_{10}^{14}\text{N}$ vs. $\log_{10}^{15}\text{N}$ (Figure 2a) exhibits a nearly perfect relationship ($r^2 = 1.0$ when rounded to 5 decimal places). Since isotopic ratios have important differences that are often detected in the 3rd, 4th or 5th decimal place and the size of subjects (and total isotope) being evaluated may vary by several orders of magnitude, almost all of the variation in a plot of common or total isotopes vs. rare isotope is due to changes in size. Therefore, exceptionally high r^2 values are to be expected in isotopic research. Since relationships are so strong, very subtle differences between slopes and y-intercepts can be statistically detected.

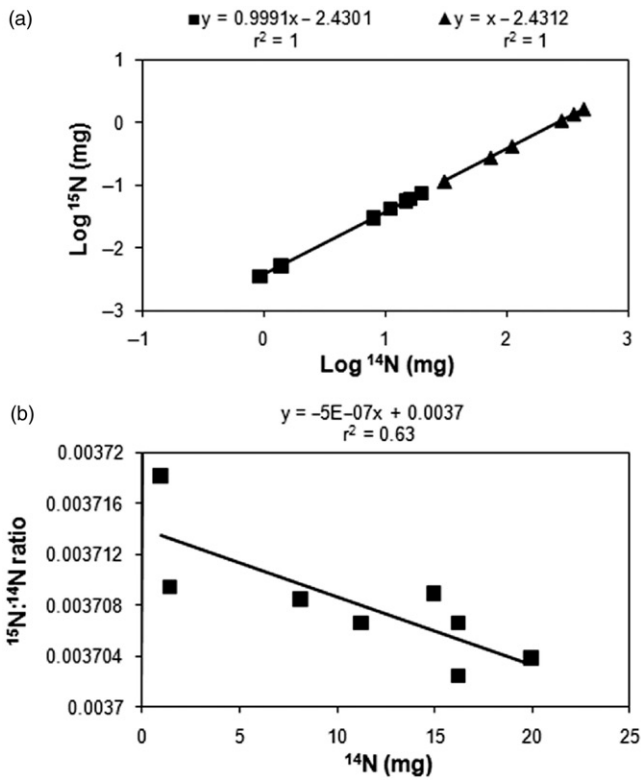


Figure 2. Scaling relationships for ^{15}N and ^{14}N in mussel. (a) $\text{Log}_{10}^{14}\text{N}$ vs. $\text{log}_{10}^{15}\text{N}$ for *Septifer vigrutus* (\blacksquare) and *Mytilus edulis* (\blacktriangle) species of mussel, data for one of which scales. (b) Relationship between $^{15}\text{N}:^{14}\text{N}$ ratio and ^{14}N (mussel size) for the scaling species (*Septifer vigrutus*). Data derived from δ values from Minagawa and Wada [23].

When species are plotted individually, ^{15}N scales with ^{14}N for the smaller species ($b = 0.9991 \pm 0.0006$, 95% C.I.), but there is isometric scaling for the larger species ($b = 1.0000 \pm 0.0004$, 95% C.I.). Total N and $\delta^{15}\text{N}$ data from the original reference were used to determine the total mass of ^{15}N . The initial total N and $\delta^{15}\text{N}$ values for the two species immediately after the experiment was initiated were not used.

Although b is only slightly less than 1.0 for *S. vigrutus*, it still suggests significant variation in $^{15}\text{N}:^{14}\text{N}$ ratios with total N. This emphasizes that seemingly negligible scaling effects can affect the interpretation of ratio-based expressions. The $^{15}\text{N}:^{14}\text{N}$ ratio (Figure 1b) decreased with size for the smaller species *S. virgutus*. Although the ratio differences in Figure 1b appear small, they are algebraically equivalent to the δ value range of 7.87–12.12 in the original reference [21].

For many scientists, it is counterintuitive to believe that miniscule deviations from isometric scaling can alter interpretation. However, it is mathematically inconsistent to ‘not believe’ that the linear y -intercepts significantly differ from zero or to ‘not believe’ the log-log slopes differ from 1.0, without also challenging the fact that the ratio is, indeed, statistically related to its denominator. The relationships are algebraically linked. When isotopic ratios are converted to the equivalent ratio-based expressions, the calculated differences are in the ranges that are generally reported in the isotopic literature.

If the scaling effect is ignored and it is assumed that ^{15}N discrimination is independent of body size, then the difference in $\delta^{15}\text{N}$ values between the two species (9.38 for *S. virgatus* vs. 8.75 for *M. edulis*) is not statistically significant ($p < 0.22$ for a two-sample t-test). P values implying that slopes and y -intercepts for the two species were significantly different (the larger species, *M. edulis*, appears to have a steeper slope) approach statistical significance ($p < 0.075$ and 0.10 for slopes and intercepts, respectively). In an analysis of covariance of $\log_{10}(^{15}\text{N})$ with $\log_{10}(^{14}\text{N})$ as a covariate, the species $\times \log^{15}\text{N}$ interaction was significant ($p < 0.014$), implying that *M. edulis* accumulates more ^{15}N as ^{14}N increases than does *S. virgatus*, even though its overall $^{15}\text{N}:^{14}\text{N}$ ratio is similar (actually slightly but not significantly less).

We can conclude that the change in ^{15}N as ^{14}N increases is different between the two species, which in a broader sense means that there are significant species differences [29]. The two species have a significant difference in ^{15}N discrimination, which was originally obscured by allometric scaling because size differences between the species were not accounted for in the scaling species. The x^2 term for a polynomial fit of the relationship between ^{15}N and ^{14}N was not statistically significant for either individual or combined species.

3.3 Scaling occurs in the accumulation of ^{13}C relative to ^{12}C

Hubick *et al.* [22] found a negative relationship between dry matter production and $\Delta^{13}\text{C}$ of peanut (*Arachis hypogaeae*) cultivars. Discrimination was lower ($^{13}\text{C}:^{12}\text{C}$ ratios higher) for the largest peanut cultivar. Conversely, Condon *et al.* [23] saw a positive relationship between biological yield and $\Delta^{13}\text{C}$ for wheat (*Triticum aestivum*) cultivars.

We suspected that, although $^{13}\text{C}:^{12}\text{C}$ ratios change in opposite directions as size (and total ^{12}C) increases, it is likely that the incremental change in ^{13}C as ^{12}C increases is similar in the two species. We re-evaluated these studies to determine whether scaling relationships might explain why large plants differ from small plants and why the sign of the relationship between ratios and their denominators differ. Total ^{13}C and total ^{12}C for individual points were derived from the original dry weight and $\Delta^{13}\text{C}$ values. Total carbon concentrations of 42% dry matter for peanut [30] and 50% for wheat were used to make the calculations. However, using any realistic estimate of total carbon concentration (40–60%) does not affect the conclusions presented in Table 2.

In this example, plots of ^{12}C vs. ^{13}C with a non-zero y -intercept; $\log_{10}^{12}\text{C}$ vs. $\log_{10}^{13}\text{C}$ plots with a slope not equal to 1.0; or ^{12}C vs. $^{13}\text{C}:^{12}\text{C}$ ratio plots are statistically significant. This suggests that scaling occurs. As discussed below, points for peanut cultivars all fall on the same allometric ^{12}C vs. ^{13}C regression line. To fully characterize scaling relationships in the wheat, replicate data from individual cultivar subpopulations would be required. However, the data does suggest that the mean isotopic ratios are related to denominator size in both species. The r^2 values in Table 2 are again exceptionally high (1.0 when rounded to 5 decimal places).

There is a significant relationship between $^{13}\text{C}:^{12}\text{C}$ ratios and total ^{12}C for both plant types. Large wheat plants (with more total isotope) appear to discriminate against the heavy isotope, while large peanut plants appear to prefer the heavy isotope relative to the smaller plants. The largest peanut cultivar (cultivar 3) has significantly higher $^{13}\text{C}:^{12}\text{C}$ ratios than the other two cultivars ($p < 0.0083$ compared to cultivar 1 and $p < 0.016$ compared to cultivar 2).

Table 2. Scaling effects on $^{13}\text{C} : ^{12}\text{C}$ ratio in wheat (*Triticum aestivum*) and peanut (*Arachis hypogaea*). Linear relationships between ^{13}C (y-axis) and ^{12}C (x-axis) with a non-zero y-intercept or linear $\log_{10} ^{12}\text{C}$ vs. $\log_{10} ^{13}\text{C}$ relationships with a slope not equal to 1.0 suggest that scaling occurs. Significant scaling then suggests that $^{13}\text{C} : ^{12}\text{C}$ ratios are dependent on denominator size and interpreting the ratio can be misleading. Data derived from $\Delta^{13}\text{C}$ values and total dry weight in Hubick *et al.* [22] and Condon *et al.* [23].

Plant	^{12}C vs. ^{13}C			$\log_{10} ^{12}\text{C}$ vs. $\log_{10} ^{13}\text{C}^z$			^{12}C vs. $^{13}\text{C} : ^{12}\text{C}$		
	Intercept	Slope	r^2 value	Intercept	Slope	r^2 value	r^2 value	r^2 value	p value
Wheat	0.000145 ^y (0.00006 – 0.00023) ^w	0.010925	1.0 ^x	-1.9588 (0.9961 – 0.9993)	0.9977*	1.0	0.315	(0.0053)	
Peanut	-0.000250* (-0.00001 – -0.00049)	0.010954	1.0	-1.9628 (1.0014* – 1.0023)	1.0014* (1.0005 – 1.0023)	1.0	0.715	(0.0040)	

^zLog-log plots with slopes not equal to 1.0 suggest that ratios allometrically scale with their denominators, but they do not necessarily suggest biological scaling curvature. An evaluation for curvature in untransformed data sets with either polynomial (significant x^2 term) or intercept inclusive power functions (scaling exponent not equal to 1.0) should accompany standard evaluations of log-log slopes.

^yp values are in parentheses.

^xAn asterisk indicates that y-intercepts for linear plots are significantly different than zero or slopes for log-log plots are significantly different than 1.0 ($p < 0.05$).

^wr square values are rounded from five decimal places.

^vValues in parenthesis represent 95% confidence limits for y-intercepts significantly different than zero or slopes significantly different than 1.0.

Interpretations of ratio-based isotopic expressions are confounded. Based on average $\delta^{13}\text{C}$, researchers have no way of knowing if large plants accumulate more, less or the same ^{13}C when evaluated on an equal-size basis than small plants. Apparent differences could be simply associated with plant size differences. Evaluating the relationship between total ^{12}C vs. ^{13}C or $\log_{10} ^{12}\text{C}$ vs. $\log_{10} ^{13}\text{C}$ as ^{12}C increases provides a better evaluation of how the accumulation of a rare isotope changes with crop type or cultivar than an isotopic ratio. Conducting an ANCOVA on ^{13}C with ^{12}C as a covariate (or $\log_{10} ^{13}\text{C}$ with $\log_{10} ^{12}\text{C}$ as a covariate) avoids biases that occur due to different plant size.

Scaling may explain the differences in isotopic ratios between large plants and small plants. The two plant types (peanut and wheat) produce parallel regression lines for the ^{12}C vs. total ^{13}C relationships. The slopes are not significantly different (Table 2). However, the two linear equations have significantly different y -intercepts. We get opposite conclusions when comparing large and small plants within the peanut and wheat cultivars only because one study produces a positive y -intercept (with corresponding log-log slope less than 1.0) while the other produces a negative y -intercept (with corresponding log-log slope greater than 1.0). The two species mathematically scale in opposite directions.

An ANCOVA can be conducted for peanut. Whether either linear or log-log models are used, covariance analyses suggest differences among peanut cultivars are indirect and related to total isotope composition rather than due to other causes. The probability level for ^{13}C cultivar differences when ^{12}C is a covariate is 0.13; differences among cultivars also change. The cultivar with the smallest original $^{13}\text{C}:^{12}\text{C}$ ratio has the greatest covariate adjusted ^{13}C accumulation. If the $\log_{10} ^{13}\text{C}$ is evaluated with $\log_{10} ^{12}\text{C}$ as a covariate, the p value for cultivar differences is 0.21 with a covariate adjusted ^{13}C order among cultivars that is similar to the untransformed ANCOVA adjusted cultivar order. In all cases there are no significant treatment \times covariate interactions.

Although changes in isotopic ratio are dependent on the fact that the two plant systems can be described by equations that scale in opposite directions, there is subtle curvature in the apparent linear relationships. The relationship between ^{12}C and ^{13}C is described by concave polynomial equations for both peanut and wheat (p values for x^2 term of 0.05 and 0.12 respectively). The derivative ($d^{13}\text{C}/d^{12}\text{C}$) for both plant types increases with ^{12}C (data not shown) even though the peanut $^{13}\text{C}:^{12}\text{C}$ ratio increases with increasing ^{12}C while the wheat $^{13}\text{C}:^{12}\text{C}$ ratio declines with increasing ^{12}C . The slope might change because size differences are related to increased photosynthesis (or some other mechanism) that results in preferential uptake of ^{12}C . However, unless slopes are evaluated, this possibility remains undetected. Intercept-related scaling effects play a much greater role with respect to how ratios differ than the subtle curvature in the data. Using a curvilinear function in an ANCOVA does not change the results presented above (data not shown).

We conclude that, although $^{13}\text{C}:^{12}\text{C}$ ratios change in opposite directions as size (and total ^{12}C) increases, the incremental change in ^{13}C as ^{12}C increases could be similar in the two species. Peanut cultivars do not differ when evaluated on a similar-size basis and replicate points fall on the same allometric total ^{12}C vs. total ^{13}C regression line. For the data that we have, mean values for wheat cultivars and all replicate points for peanut fall on parallel allometric regression lines. Whether or not replicate points for wheat cultivars fall on the same or different regression lines could not be determined. Although wheat cultivars generally have more ^{13}C than peanut cultivars on an equal ^{12}C basis, any incremental change differences in ^{13}C as ^{12}C increases in the two genera remain unknown.

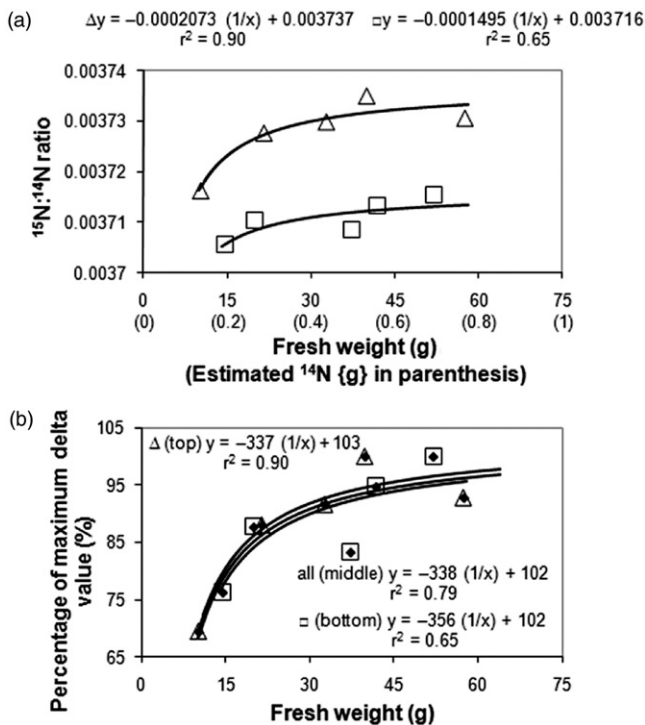


Figure 3. Scaling relationships for ^{15}N and ^{14}N within food source treatments. (a) Relationship between $^{15}\text{N}:^{14}\text{N}$ ratio and fresh weight for Dover sole (*Microstomus pacificus*) grown in polluted (\square) and unpolluted (Δ) costal sites. Values for total ^{14}N that were derived from water content and N concentration estimates are shown in parenthesis. Data derived from δ values from Rau *et al.* [24]. (b) The same data presented in a, but the $^{15}\text{N}:^{14}\text{N}$ ratio has been expressed as a percentage of maximum delta value for each individual costal site.

3.4 Effects due to both treatment and scaling for the accumulation of ^{15}N relative to ^{14}N

In this example, we demonstrate how scaling could either obscure or magnify treatment differences in an isotopic ratio. Statistically significant relationships between $^{15}\text{N}:^{14}\text{N}$ ratio and fresh weight for Dover sole (*Microstomus pacificus*) grown in polluted and unpolluted costal sites are presented in Figure 3a. Data were derived from δ values from Rau *et al.* [24]. The $^{15}\text{N}:^{14}\text{N}$ ratios shown in the figure are algebraically equivalent to δ values of 8.7–11.4 and 11.6–15.5 for respective polluted and non-polluted sites. Estimates for total ^{14}N derived from moisture content and N concentration estimates are shown in parenthesis. Isotopic ratios when analyzed with or without dry weight as a covariate are statistically different ($p < 0.01$) for the two sites. The $\log_{10}^{14}\text{N}$ vs. $\log_{10}^{15}\text{N}$ and ^{14}N vs. ^{15}N regression lines are not statistically different for polluted and unpolluted sites, but even with only five points for each regression line, slope and y -intercept differences for the linear equations representing the two sites approach statistical significance (^{14}N vs. ^{15}N slope differences; $p < 0.09$). However, in an ANCOVA analysis of ^{15}N with ^{14}N as a covariate there is a treatment \times ^{14}N interactions ($p < 0.009$). The change in ^{15}N as ^{14}N increases is different between the two conditions. As would be expected if food sources differ, the non-polluted site has both higher ratios and an apparently steeper slope.

Since fish sizes at both sites are similar, the scaling does not interfere with a ratio-based assessment of isotopic differences. However, if a small fish (10g) from the unpolluted site were compared to a large fish (70 g) from the polluted site, scaling would obscure the isotopic discrimination that is revealed in ratio-based expressions. If a large fish from the unpolluted site were compared to a small fish from the polluted site, scaling would magnify differences in the isotopic ratio. Rau *et al.* [24] are correct in suggesting that growth, animal size and metabolism differences can likely alter isotopic composition.

In Figure 3b, the $^{15}\text{N}:^{14}\text{N}$ ratio has been expressed as a percentage of maximum delta value for each individual coastal site. Again, the data clearly show that isotopic ratios scale with body size. The x^2 term for a polynomial fit of the relationship between ^{15}N and ^{14}N was not statistically significant for the polluted or unpolluted data sets.

3.5 Scaling complicates ^{15}N interpretation for different trophic levels

The following data demonstrate why total isotope, although rarely measured in trophic level studies, should be statistically evaluated. When mean estimates of common isotope (x -axis) are plotted against mean estimates of rare isotope (y -axis) for trophic level studies, a concave curvilinear function with a positive scaling exponent is expected. This is not surprising. The isotopic ratio increases with body size as bigger animals with more total isotope eat bigger prey with larger rare isotope : common isotope ratios. It is probably not realistic to assume that the collection of points from which the mean values are determined is isometric within a species. This would imply that scaling is isometric within a species while it is allometric between them [16]. Without replicate total common and rare isotope data, it is impossible to determine if points for different species will fall on common or different allometric regression lines. Thus one cannot detect isotopic differences among trophic levels that are independent of the size of the animals being evaluated.

Jennings *et al.* [18] were concerned about size-related factors that alter isotopic composition and present sufficient data for a scaling analysis. Figure 4a displays the animal size vs. $\delta^{15}\text{N}$ relationships for three (zooplankton, small fish, large fish) of five faunal groups from one of their original figures. The mean $\delta^{15}\text{N}$ value for the zooplankton differs from both small and large fish ($p < 0.0001$). Although large fish tend to have higher $\delta^{15}\text{N}$ than small fish, this difference is not statistically significant ($p < 0.265$). However, as discussed below, differences or lack of differences in isotopic ratio do not necessarily provide information on how different sized faunal groups accumulate ^{15}N .

When plotted on a linear scale (Figures 4b and 4c) scaling within each faunal group is clearly apparent. This might be expected if increasing animal size is associated with increasing prey size, thus both increasing animal size and increasing $\delta^{15}\text{N}$ reflect changing trophic levels. When the differences in N:C ratio (that were presented in the original reference) and realistic assumptions from the literature for C concentration for the three faunal groups are evaluated, log-log and traditional non-transformed regressions can be evaluated (Table 3). Scaling is clearly apparent. Negative y -intercepts in the non-transformed data were statistically significant for the zooplankton and negative y -intercepts approach statistical significance ($p < 0.1$) for both fish species. For all three faunal groups, log-log scaling exponents were statistically different than 1.0.

As was the case in Figure 2a and Table 2, r^2 values presented in Table 3 are exceptionally high (1.0 when rounded to 8 decimal places). Since ^{15}N isotopic ratios vary over an even smaller range than ^{13}C isotopic ratios, and animal size varies more (several

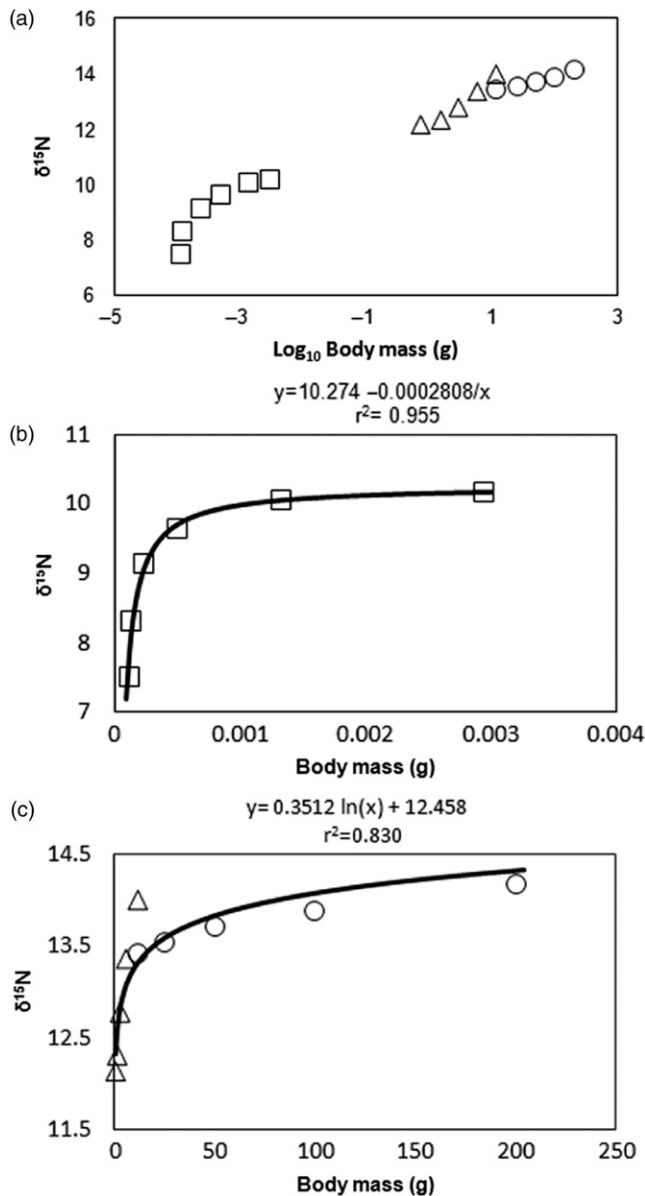


Figure 4. Trophic level scaling relationships for ^{15}N and ^{14}N . (a) Relationship between $\delta^{15}\text{N}$ and body mass ($\log_{10}M$, midpoints of wet mass classes) for the sampled faunal groups (\square) zooplankton, (\triangle) small fish and (\circ) large fish. (b) Relationship between $\delta^{15}\text{N}$ and body mass for zooplankton. (c) Relationship between $\delta^{15}\text{N}$ and body mass for (\triangle) small fish and (\circ) large fish. Data derived from Jennings *et al.* [18].

orders of magnitude in some cases) than in the plant example (Table 2), r^2 values are even higher than what was previously reported.

The 95% confidence intervals for the log-log slopes for zooplankton overlap with both small and large fish. However, confidence levels for log-log slopes for small and

Table 3. Scaling relationships for zooplankton, large fish and small fish. Linear relationships between ^{15}N (y-axis) and ^{14}N (x-axis) with a non-zero y-intercept or $\log_{10}^{14}\text{N}$ vs. $\log_{10}^{15}\text{N}$ plots with a slope not equal to 1.0 suggest that scaling occurs. Data derived from Jennings *et al.* [18].

Fauna	Total ^{14}N vs. total ^{15}N			\log_{10} total ^{14}N vs. \log_{10} total $^{15}\text{N}^z$		
	Intercept (95% CI)	Slope (95% CI)	r^2 value ^y (p value) ^x	Intercept (95% CI)	Slope (95% CI)	r^2 value (p value)
Zooplankton	$-1.048 * 10^{-11}$ ($\pm 1.87 * 10^{-12}$)	0.003697 ($\pm 1.09 * 10^{-7}$)	1.0 (< 0.001)	-2.42906 (± 0.002453)	1.0006577 (± 0.0004754)	1.0 (0.0015)
Small fish	$-1.7108 * 10^{-7}$ ($\pm 1.97 * 10^{-7}$)	0.003712 ($\pm 2.11 * 10^{-6}$)	1.0 (0.070)	-2.43004 (± 0.00377)	1.0006712 (± 0.0002673)	1.0 (< 0.001)
Large fish	$-1.3286 * 10^{-6}$ ($\pm 1.72 * 10^{-6}$)	0.003712 ($\pm 9.50 * 10^{-7}$)	1.0 (0.091)	-2.42890 (± 0.0000362)	1.0002593 (± 0.0000083)	1.0 (< 0.001)
All three groups	$-2.8259 * 10^{-7}$ ($\pm 3.53 * 10^{-7}$)	0.003711 ($\pm 3.36 * 10^{-7}$)	1.0 (0.109)	-2.43049 (± 0.0001471)	1.000391 (± 0.0000435)	1.0 (< 0.001)

^zLog-log plots with slopes not equal to 1.0 suggest that ratios allometrically scale with their denominators, but they do not necessarily suggest biological scaling curvature. An evaluation for curvature in untransformed data sets with either polynomial (significant x^2 term) or intercept inclusive power functions (scaling exponent not equal to 1.0) should accompany standard evaluations of log-log slopes.

^y r^2 values are rounded to the eight decimal places.

^xp values shown are for intercept not equal to 0 for linear equations and slope not equal to 1.0 for log-log equations.

large fish differ. Small fish have a larger log-log slope and a similar y -intercept than large fish, suggesting that they would accumulate more ^{15}N on an equal total isotope basis. There is statistically detectable concave curvature (significant positive x^2 terms for polynomial best fit equations) for the raw data for fish shown in Table 3. For the non-transformed small and large fish, derivatives increase with increasing ^{14}N (x^2 p values = 0.0165 and 0.00116 respectively for small and large fish). If the data are fit to a power function with an intercept term, scaling exponents become larger with greater statistical significance than the simpler log-log equations for the fish in Table 3. The best-fit polynomial and intercept inclusive power functions both suggest that within a fish group, there is indeed, a greater preference for ^{15}N accumulation as size increases.

The significant scaling apparent in the log-log slopes (Table 3) for zooplankton is likely due to positive y -intercepts. Log-log plots with slopes not equal to 1.0, in themselves, do not necessarily suggest that nonlinear biological scaling occurs. An evaluation for curvature in an original untransformed data set with either polynomial (significant x^2 term) or intercept inclusive power functions (scaling exponent not equal to 1.0) should accompany standard evaluations of log-log slopes. Both polynomial best fit (x^2 p value < 0.589) equations and scaling exponents for intercept inclusive power functions that are not significantly different than 1 suggest a lack of curvature in the zooplankton data.

For zooplankton, the fact that $\delta^{15}\text{N}$ increases over time [18] suggests that data could come from a perturbed system where the $\delta^{15}\text{N}$ of the primary food source has increased. In this perturbed system, smaller animals with faster metabolism could approach a new equilibrium faster than larger animals. Under these conditions, metabolism based scaling would cause small animals to have larger $\delta^{15}\text{N}$, while trophic level based scaling would cause small animals to have a lower $\delta^{15}\text{N}$. Other possible mechanisms could also explain a linear total ^{14}N vs. total ^{15}N function that has a negative y -intercept.

The relationship for zooplankton shown in Figure 3b is difficult to interpret. Even though the ratio changes, there is no change (^{14}N vs. ^{15}N slope is constant) in how ^{15}N incrementally accumulates relative to ^{14}N as body size increases. The significant differences suggested by standard deviations for $\delta^{15}\text{N}$ that do not overlap (Jennings *et al.* 2008) for zooplankton in different size categories do not necessarily reflect differences in how the ^{15}N is accumulated as total isotope increases. Again it is unlikely that common isotope vs. rare isotope relationships are isometric within a size category but allometric between them. Without an analysis of replicate data for the individual zooplankton size categories, we have no idea if isotopic ratios differ independent of size. Points could fall on either the same or different allometric regression lines for the different assortment of species that likely occur in the different size categories.

Comparing different-sized fish categories is also more complex than what the mean $\delta^{15}\text{N}$ values suggest. Both the small fish and large fish have similar non-transformed slopes ($^{14}\text{N} \times$ fauna type interaction; $p < 0.958$), but the large fish have a more negative y -intercept and significantly lower covariate adjusted ^{15}N ($p < 0.03$ after insignificant fish size \times total isotope interactions are removed from the model) than the small fish. Ratio-based isotopic evaluations are misleading. Based on average $\delta^{15}\text{N}$, a researcher would have no way of knowing that the large fish accumulate less ^{15}N when evaluated on an equal- ^{14}N basis than the small fish. Scaling masks a treatment effect. If size were the only factor contributing to trophic level differences, one would expect greater $^{15}\text{N}:^{14}\text{N}$ ratios for larger fish, while the two size categories would have similar ^{15}N when total ^{14}N is used as a covariate in an ANCOVA.

Regardless of the cause of observed scaling, evaluating changes in the slope for a plot of total ^{14}N vs. total ^{15}N as body size increases and conducting an ANCOVA to evaluate treatments with different amounts of total isotope will give a better measure of how the accumulation of a rare isotope differs than an isotopic ratio.

3.6 Recognising confounded systems that produce a combination of difficult to separate direct and indirect effects

We present global carbon data to demonstrate how changing conditions can induce scaling effects that complicate the interpretation of other ongoing analyses. Unlike many less-studied systems, both total isotope and ratio-based isotopic expressions are available. Nothing we present alters isotopic global carbon interpretations. However, this example demonstrates how slope analyses and an evaluation of curvature in common or total isotope vs. rare isotope plots are useful tools in efforts to better understand isotopic data.

Since fossil fuels have an isotopic composition that is more depleted in ^{13}C than the atmosphere, increased fossil fuel consumption results in declining $\delta^{13}\text{C}$ values over time [31,32]. Without complicating factors, carbon added to the atmosphere would have $\delta^{13}\text{C}$ values that reflect fossil fuel input, which has varied from about -24 to -29 over the industrial era [33]. However, discrimination among isotopes as CO_2 is removed by photosynthesis, different isotopic composition of the CO_2 that is added from respiration and oceanic interactions change the isotopic composition of added CO_2 [31,32].

Past Keeling plot analyses from the Law Dome ice core suggest that the long-term historic isotopic composition of added carbon in delta value equivalents is approximately -13 to -14 [34]. If all the complicating factors are relatively constant over time, changes in the rate of fossil fuel addition to the atmosphere might be revealed by evaluating slope changes in total CO_2 (or $^{12}\text{CO}_2$) vs. $^{13}\text{CO}_2$ plots. As the emission rate increases, the isotopic composition of added CO_2 would become more depleted. As the rate decreases the isotopic composition would become more enriched.

As both the rate of fossil fuel emissions per year [35] and the $\delta^{13}\text{C}$ of the fuel source increase [33], a plot of total CO_2 vs. $^{13}\text{CO}_2$ in the atmosphere (as inferred from Antarctic ice core and firn samples) can be generally described by a convex polynomial function. The fact that $^{13}\text{CO}_2$ and total CO_2 co-vary in a simple-to-parameterise way simply means that the system has a relatively constant set of sources and sinks. The progressive slope change can be seen in the equations presented in Table 4 for data collected by Francey *et al.* [27] and Friedli *et al.* [28]. A changing environment with increasing CO_2 concentration eventually creates a scaling system where linear or log-log plots of total CO_2 vs. $^{13}\text{CO}_2$ statistically scale. Therefore after 1905, $\delta^{13}\text{C}$ values can decline regardless of whether the isotopic composition of the CO_2 being added to the atmosphere becomes slightly more enriched, less enriched, or remains constant.

An example of a convex polynomial is shown in Table 5 for 1940–1978. However, there is an anomaly for the time period from 1978 to 1993 (Table 5). The ice core and firn data can be described by a statistically significant concave polynomial regression equation during this short recent time interval, suggesting that the CO_2 being added to atmosphere was becoming more rather than less enriched in ^{13}C .

The $d^{13}\text{CO}_2/d$ total CO_2 derivative also increases during this time (data not shown). The concave equation describes the data even though the atmosphere as a whole is becoming more depleted. A similar concave polynomial equation (also presented

Table 4. $^{13}\text{CO}_2$ and total CO_2 atmospheric scaling relationships over the last 150 years. Linear relationships between $^{13}\text{CO}_2$ (y -axis) and total CO_2 (x -axis) with a non-zero y -intercept or linear $\log_{10}^{12}\text{CO}_2$ vs. $\log_{10}^{13}\text{CO}_2$ relationships with a slope not equal to 1.0 suggest that scaling occurs. The r^2 values for all equations are 1.0 when rounded to five decimal places. Data derived from Keeling *et al.* [25], Keeling *et al.* [26], Francey *et al.* [27], Friedli *et al.* [28], Blasing *et al.* [33] and Marland *et al.* [42].

Data source and date interval	n	Fossil fuel delta $^{13}\text{C}^z$	Total CO_2 vs. $^{13}\text{CO}_2$	\log_{10} total CO_2 vs. $\log_{10}^{13}\text{C}^y$
Combined Law ice dome and Siple ice core				
1840–1882	6	-24.11	$^{13}\text{CO}_2 = 0.011033 \text{ tot CO}_2 + 0.012913$	$\log^{13}\text{CO}_2 = 0.99596 \log \text{ tot CO}_2 - 1.94080$
1882–1905	8	-24.28	$^{13}\text{CO}_2 = 0.011066 \text{ tot CO}_2 + 0.003218$	$\log^{13}\text{CO}_2 = 0.99902 \log \text{ tot CO}_2 - 1.94833$
1905–1940	14	-24.74	$^{13}\text{CO}_2 = 0.011014 \text{ tot CO}_2 + 0.018604^{*x}$	$\log^{13}\text{CO}_2 = 0.99432^* \log \text{ tot CO}_2 - 1.93675$
1940–1978	17	-27.20	$^{13}\text{CO}_2 = 0.010997 \text{ tot CO}_2 + 0.023910^*$	$\log^{13}\text{CO}_2 = 0.99322^* \log \text{ tot CO}_2 - 1.93402$
Antarctic air firn1 + 2 1978–1993	55	-28.31	$^{13}\text{CO}_2 = 0.011005 \text{ tot CO}_2 + 0.020751^*$	$\log^{13}\text{CO}_2 = 0.99462^* \log \text{ tot CO}_2 - 1.9423$
Point Barrow air 1982–1997	43 ^w	-28.67	$^{13}\text{CO}_2 = 0.010991 \text{ tot CO}_2 + 0.024558^*$	$\log^{13}\text{CO}_2 = 0.99380^* \log \text{ tot CO}_2 - 1.9404$

^zEstimates for fossil fuel $\delta^{13}\text{C}$ values were calculated as a weighted average of the mean fossil fuel contributions and $\delta^{13}\text{C}$ values for each year. Delta ^{13}C values for each year were estimated as presented by Blasing *et al.* [33]: $\delta^{13}\text{C} = ((-24.1\text{S}) + (-26.5\text{L}) + (-40.0\text{G})) / (\text{S} + \text{L} + \text{G})$ where S, L, and G are respective values of carbon emissions for solid, liquid, and gas fossil fuel types taken from the data derived from Marland *et al.* [42]. The coefficients are best estimates of the mean $\delta^{13}\text{C}$ values for the respective fuels [33].

^yLog-log plots with slopes not equal to 1.0 suggest that ratios allometrically scale with their denominators, but they do not necessarily suggest biological scaling curvature. An evaluation for curvature in untransformed data sets with either polynomial (significant x^2 term) or intercept inclusive power functions (scaling exponent not equal to 1.0) should accompany standard evaluations of log-log slopes.

^xAn asterisk indicates a scaling equation (a ratio is dependent on denominator size) and denotes that y -intercepts are significantly different than zero for linear equations or slopes are significantly different than 1.0 for log-log equations.

^wOnly February, March and April data that was relatively stable (not changing over time) was used to determine an equation that was not affected by annual oscillation of the amount of CO_2 and its isotopic content.

Table 5. Observed polynomial relationships between $^{13}\text{CO}_2$ and total CO_2 for Antarctic ice core, Antarctic air samples and Point Barrow air samples. Statistically significant negative $(\text{CO}_2)^2$ coefficients indicate convex curvature where the amount of $^{13}\text{CO}_2$ accumulation in the atmosphere is decreasing as total CO_2 increases; Statistically significant positive $(\text{CO}_2)^2$ coefficients indicate concave curvature where the amount of $^{13}\text{CO}_2$ accumulation in the atmosphere is increasing as total CO_2 increases. Data derived from Keeling *et al.* [25], Keeling *et al.* [26] and Francey *et al.* [27].

Data type	n	Date interval	Total CO_2 vs. $^{13}\text{CO}_2$	P value for χ^2 term
Law ice dome	18	1940–1978	$^{13}\text{CO}_2 = -2.905 * 10^{-6}(\text{tot CO}_2)^2 + 0.0128(\text{tot CO}_2) - 0.2734$	0.0202
Antarctic firm 1 + 2	55	1978–1993	$^{13}\text{CO}_2 = 1.010 * 10^{-6}(\text{tot CO}_2)^2 + 0.0103(\text{tot CO}_2) + 0.0143$	0.0035
Point Barrow	43 ^z	1983–1997	$^{13}\text{CO}_2 = 2.530 * 10^{-6}(\text{tot CO}_2)^2 + 0.0092(\text{tot CO}_2) + 0.3496$	0.0030

^zOnly February, March and April data that were relatively stable (not changing over time) were used to determine an equation that was not affected by annual oscillation of the amount of CO_2 and its isotopic content.

in Table 5) is revealed when Point Barrow air samples [25,26] are evaluated for 1983–1997. This is in agreement with the conclusions of Gruber *et al.* [36] where $\delta^{13}\text{C}$ changes for 1980–1995 in both the atmosphere and the ocean are attributable to a deceleration in the growth of anthropogenic CO_2 emissions after 1979. An increasing slope could also be caused by decreases in CO_2 inputs from terrestrial respiration.

A changing slope (implied by the polynomial equations in Table 5) or derivative is clearly more revealing than changes in $\delta^{13}\text{C}$ for 1978–1997. Since they more clearly reveal changes in source-sink relationships, slopes or derivatives will better represent system change in a scaling system than $\delta^{13}\text{C}$. Scaling effects could also complicate the interpretation of the seasonal oscillation in $\delta^{13}\text{C}$ values that occur in the Northern hemisphere.

Seasonal oscillations are presented in Figure 5a [25] in which the long term decrease of $^{13}\text{CO}_2$: total CO_2 ratios has been removed. These oscillations can be statistically associated with changes in respiration and photosynthesis. A statistically significant convex polynomial equation describes the combined data pooled across all months ($^{13}\text{CO}_2 = -2.080 \cdot 10^{-6} [\text{total CO}_2]^2 + 0.01229 [\text{total CO}_2] - 0.1758$; $r^2 = 0.999989$; x^2 term significant $p < 0.0008$). As CO_2 increases when respiration is dominant, CO_2 becomes more depleted; as CO_2 declines with increased photosynthesis and levels return to their minimum, CO_2 becomes more enriched.

In a scaling system, the addition to or removal of CO_2 in the atmosphere will change $\delta^{13}\text{C}$ values regardless of whether or not these additions are associated with changes in the isotopic composition of the CO_2 that is added or removed. Therefore, we would expect part of the magnitude of the observed oscillation is attributable to a scaling effect. Modelled results in Figure 5b show both the total oscillation observed and the scaling effect.

The two curves in Figure 5b were constructed by using the year-adjusted values for CO_2 concentrations presented by the original authors [25,26]. Values for the modelled total $^{13}\text{CO}_2$: total CO_2 ratio oscillation were derived by assuming that the isotopic composition of added or removed CO_2 was defined by the polynomial best-fit equation (presented above) that described the relationship between total CO_2 and $^{13}\text{CO}_2$ for the year-adjusted monthly data over the 15-year time period.

Values for the scaling effects were derived by assuming that the isotopic composition of added or removed CO_2 remained unchanged (a delta value equivalent of -14) as CO_2 increased or decreased and represent a stable source for added CO_2 over the 15-year period. Our model where the isotopic composition of the CO_2 added to and removed from the atmosphere are identical is not necessarily realistic. However, the simulation does demonstrate how unchanging isotopic content of additions and losses will lead to changes in an isotopic ratio. Our value of -14 is derived from the slope of the $^{12}\text{CO}_2$ vs. $^{13}\text{CO}_2$ plot for the 15-year time period when only Feb, March and April data were evaluated. By restricting data to these relatively stable times, the equation is not affected by annual oscillations of the amount of CO_2 and its isotopic content.

Both the real and artificial data have similar oscillation magnitudes for the $^{13}\text{CO}_2$: total CO_2 ratio. Most of the change observed in Figure 5a is due to a change in the composition of the CO_2 being added or removed, but a scaling factor also plays a role (Figure 4b). In many systems, changes in a ratio can be due to a combination of treatment and scaling effects.

In Figure 5c, modelled results show theoretical patterns of change in the amplitude of cyclic seasonal ^{13}C isotopic composition in the atmosphere from 1840–1997. A model was used because historic data over the entire time period is not available and a variety of

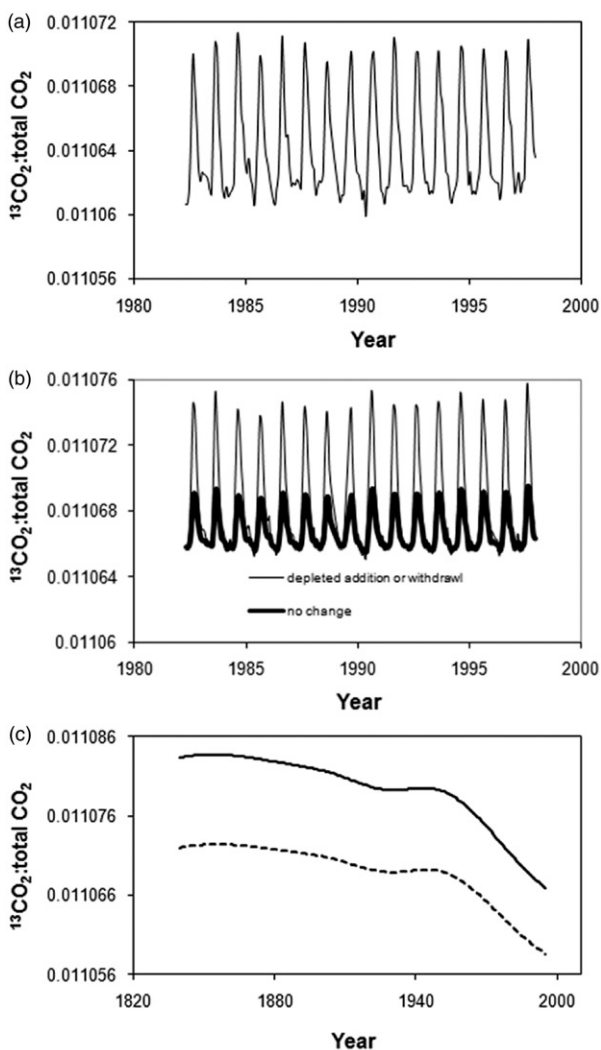


Figure 5. Modelled and observed cyclic seasonal ^{13}C isotopic composition for Point Barrow, Alaska air samples for the late 20th century and modelled long-term changes in the cyclic rise and fall of ^{13}C isotopic composition of the atmosphere from 1840–1997. (a) Seasonal changes for $^{13}\text{CO}_2:\text{total CO}_2$ ratio after removing trends for long-term change. Data were created by using spline-smoothed, year-adjusted data. (b) Modelled annual change that would occur if the cyclic rise and fall in CO_2 added to the atmosphere had no change (in bold) in CO_2 source ($\delta^{13}\text{C} = -14$) and modelled annual change that would occur if the CO_2 added to or removed from the atmosphere was subject to source changes associated with respiratory additions of depleted ^{13}C and selective removal of ^{12}C by photosynthesis (standard line). (c) Modelled change in the amplitude (— maximum value; ---- minimum value) of cyclic seasonal ^{13}C isotopic composition of the atmosphere from 1840–1997. Data after Keeling *et al.* [25], Keeling *et al.* [26], Francey *et al.* [27], and Friedli *et al.* [28].

factors that alter oscillation patterns may obscure a scaling effect. However, it is important to recognize the underlying scaling effect that must mathematically exist.

These data were produced by introducing the average oscillation of CO_2 found in Point Barrow air samples over a 15-year period [25,26] into a historic record derived from

Antarctic ice core and firn data [27,28]. Once again, the isotopic composition of cyclic additions or removal of CO_2 was defined by the polynomial best-fit equation that described the relationship between total CO_2 and $^{13}\text{CO}_2$ in the Point Barrow data set for the year-adjusted data over a 15-year time period. The amplitude decreases by 27% between 1840 and 1997 and by 19% between 1950 and 1997. Similar trends were not apparent in the amplitudes of either total CO_2 or $^{13}\text{CO}_2$ in the artificial data set. The amplitudes only declined by about 2% in the artificial data for total CO_2 or $^{13}\text{CO}_2$ between 1840 and 1997.

The model implies that, even if the amount of CO_2 that is cyclically added to and removed from the atmosphere remains constant, and even if the magnitude of the cyclic changes in isotopic composition of the CO_2 that is added or removed also remains constant, scaling effects will cause a decrease in cyclic ^{13}C : total C ratio amplitudes. When a ratio-based expression is used to quantify system change, the long-term additions of fossil fuel derived CO_2 dampen the apparent short-term oscillation attributed to changes in the isotopic composition of the CO_2 that is added to or removed from the atmosphere. Scaling effects could make it more difficult to detect an increase in the amplitude of cyclic isotopic change that could occur in response to changes in environmental conditions associated with fossil fuel additions. Trends in Figure 5 are similar if $^{13}\text{CO}_2$: $^{12}\text{CO}_2$ ratios, rather than $^{13}\text{CO}_2$:total CO_2 ratios, are plotted on the y -axes (data not shown).

Our fixed-composition flux iteration models reflect simple mass balance. Atmospheric CO_2 has a $\delta^{13}\text{C}$ of about -7 , so adding or removing carbon with a -14 $\delta^{13}\text{C}$ value is necessarily going to make the isotopic ratio co-vary with CO_2 concentration. As total pool size increases the magnitude of oscillations will decrease. In global carbon research both total carbon and isotopic ratio changes are well studied. Without the knowledge of the total CO_2 change, fluctuating isotopic ratios would be difficult to interpret. In many other systems, changes in isotopic ratio are evaluated without detailed evaluations of total isotope change. Evaluating total isotope and observing how derivatives change is a relatively simple technique that is much more revealing than studying ratio changes independent of total isotope.

Seasonal, diurnal or millennial patterns in ratio-based isotopic data are often evaluated in biological and ecological studies, but the possibility that either known or unknown factors can induce scaling effects is generally ignored. This is unfortunate since, as demonstrated both here and in the supplementary document [16], scaling effects can theoretically dampen, enhance or reverse oscillation patterns. Oscillation patterns (and other δ value changes over time) should not be evaluated without knowledge of total isotope change.

3.7 Using derivatives to estimate cyclic changes in the isotopic composition of atmospheric CO_2

A Keeling plot [20] where $\delta^{13}\text{C}$ is plotted against $1/\text{total } \text{CO}_2$, is often used to estimate the isotopic composition (y -intercept) of the respired CO_2 added to the atmosphere [34,37,38]. We advocate using derivatives as a better way to evaluate changes in the isotopic composition of substances added to or removed from a scaling system.

Keeling plots (in which the long-term, fossil fuel induced decrease of $^{13}\text{CO}_2$:total CO_2 ratios has been removed) for Point Barrow data suggest that the isotopic composition of

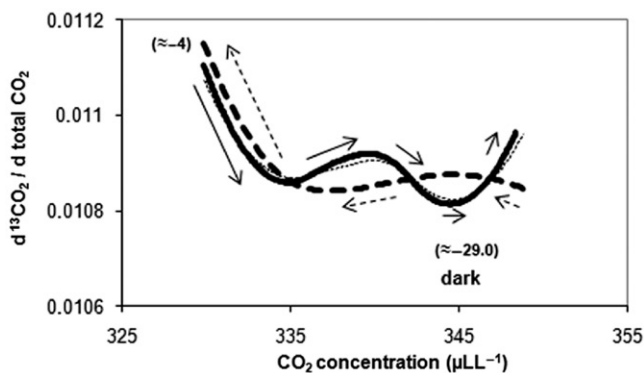


Figure 6. Derivatives ($d^{13}\text{CO}_2/d \text{ total CO}_2$) for Point Barrow, Alaska air samples for the late 20th century after removing trends for long-term change. Derivatives for all months (---), May to August (---; in bold); when photosynthesis becomes dominant and CO_2 decreased and August to April (—; in bold); when respiration becomes dominant and CO_2 increased are shown. Arrows indicate whether CO_2 is increasing (\rightarrow) or decreasing ($-\rightarrow$) as the derivative changes. Data in parenthesis are approximate $\delta^{15}\text{N}$ values derived from minimum and maximum $d^{13}\text{CO}_2/d \text{ total CO}_2$ values. Numeric derivatives were estimated using a cubic equation with 7 knots. Data after Keeling *et al.* [25] and Keeling *et al.* [26].

CO_2 added to the atmosphere by terrestrial respiration has a $\delta^{13}\text{C}$ value of about -25 [34,37]. A similar approach has been applied to other data sets producing $\delta^{13}\text{C}$ values for terrestrially respired CO_2 that range from -22.79 to -27.40 [38]. However, Nickerson and Risk [39] have suggested that Keeling plots are non-linear, violating key assumptions of the technique. Linear relationships are not expected since the isotopic composition of CO_2 added to or removed from the atmosphere changes over time.

The $d^{13}\text{CO}_2/d \text{ total CO}_2$ derivatives for both increasing and decreasing phases of CO_2 concentration are shown in Figure 6. When CO_2 concentration is approaching its highest level as respiration becomes dominant, the source becomes more depleted. The most depleted derivative occurs in the dark when photosynthesis is not possible. During photosynthesis, plants preferentially assimilate $^{12}\text{CO}_2$, resulting in an increase of $^{13}\text{CO}_2: ^{12}\text{CO}_2$ or $^{13}\text{CO}_2: \text{total CO}_2$ ratios remaining in the atmosphere. The most enriched derivative occurs in August when CO_2 concentrations have declined to their lowest level and photosynthesis is dominant. Most of the derivative change occurs during a very narrow range of total CO_2 values ($330\text{--}335 \mu\text{L L}^{-1}$), slightly before and after the time of maximum CO_2 assimilation, which corresponds to the lowest CO_2 concentration. Respiration still occurs as photosynthesis becomes more important, thus the derivative represents a combination of source and sink effects as total net CO_2 concentrations decline.

Keeling plots have expanded beyond their initial global carbon application. The approach has been applied to quantify the $\delta^{13}\text{C}$ of CO_2 being respired by hummingbirds [40] and lakes [41]. This indirect method of approximating the slope should only be used if the underlying total or common isotope vs. rare isotope relationships is known to be linear. Best-fit linear relationships with exceptionally high r^2 values may miss subtle, but important, curvature.

4. Conclusions

These examples demonstrate that interpreting statistical differences in ratio-based isotopic expressions can be fraught with difficulties. Regardless of the cause, hidden scaling can confound analysis of treatment effects. Treatments can induce scaling or a ubiquitous scaling effect can create apparent differences among treatments. One should not assume that relationships between isotopic composition and total isotope are isometric. In some situations it may be difficult to untangle a combination of ubiquitous scaling, treatment-induced scaling and direct treatment effects.

Interpreting observed differences in isotopic ratios requires an evaluation to determine whether treatments directly affect how a rare isotope is accumulated or are associated with differences in denominator size. By simply recording total elemental content, standard statistical procedures that evaluate changes in slopes or derivatives can be combined with an ANCOVA to better evaluate isotopic data. An ANCOVA on either the numerator with the denominator as a covariate; or the \log_{10} of the numerator with the \log_{10} of the denominator as a covariate is a well established alternative to statistically evaluating ratios that scale. Slope differences or derivatives are also more revealing than changes in isotopic ratios and better represent system change in a scaling system. If effects are direct, points for different treatments fall on different linear and log-log (total isotope vs. rare isotope or common isotope vs. rare isotope) regression lines.

Acknowledgements

We thank Ray William, C. J. Weiser, Neal DeVos, and George Fernandez for reviewing earlier ratio-related manuscripts and for their continued support and encouragement that eventually led to this report. We also thank Wanda Parrott for editorial assistance.

References

- [1] J. Huxley and G. Teisser, *Nature* **137**, 78 (1936).
- [2] R.H. Peters, *The Ecological Implications of Body Size* (Cambridge University Press, New York, 1983).
- [3] V.M. Savage, J. F. Gillooly, W. H. Woodruff, G.B. West, A.P. Allen, B.J. Enquist, and J.H. Brown, *Funct. Ecol.* **18**, 257 (2004).
- [4] J.H. Brown and G.B. West, *Scaling in Biology* (Oxford University Press, New York, 2000).
- [5] J.M. Tanner, *J. Appl. Physiol.* **2**, 1 (1949).
- [6] T.L. Righetti, D. Sandrock, B. Strik, and A. Azarenko, *J. Amer. Soc. Hort. Sci.* **132**, 429 (2007).
- [7] T.L. Righetti, D. Dalthorp, D. Sandrock, B. Strik, and P. Banados, *J. Hort. Sci. Biotech.* **82**, 641 (2007).
- [8] L. Kratochvil and F. Jaroslav, *Biology Letters.* **5**, 643 (2009).
- [9] K. Pearson, *Proc. R. Soc. Lond.* **60**, 489 (1896).
- [10] W.R. Atchley, C.T. Gaskins, and D. Anderson, *Syst. Zool.* **25**, 137 (1976).
- [11] G.C. Packard and T.J. Boardman, *Physiol. Zool.* **61**, 1 (1988).
- [12] E.T. Poehlman and M. J. Toth, *Am. J. Nutr.* **61**, 482 (1995).
- [13] M. Jasienski and F. A. Bazzar, *Oikos* **84**, 321 (1999).
- [14] T.L. Righetti, D.R. Sandrock, B. Strik, C. Vasconcelos, Y. Moreno, S. Ortega-Farias, and P. Banados, *J. Amer. Soc. Hort. Sci.* **132**, 3 (2007).
- [15] D. Raubenheimer and S.J. Simpson, *Entomologica Experimentalis et Applicata* **62**, 221 (1992).

- [16] T.L. Righetti, D. Sandrock, D. Dalthorp, J. Lambrinos, B. Strik, and C. Phillips, Supplementary document with conceptual examples (2010).
- [17] A.E. Carelton and C.M. del Rio, *Oecologia* **144**, 226 (2005).
- [18] S.T. Jennings, A.D. Maxwell, M. Schratzberger, and S.P. Milligan, *Mar. Ecol. Prog. Ser.* **370**, 199 (2008).
- [19] M. del Rio, N. Wolf, S.A. Carleton, and L.Z. Gannes, *Biol. Rev.* **84**, 91 (2008).
- [20] C.D. Keeling, *Geochimica Cosmochimica Acta* **24**, 277 (1961).
- [21] M. Minagawa, M. Wada, and E. Wada, *Geochim. Cosmochim. Ac.* **48**, 1135 (1984).
- [22] K.T. Hubick, R. Shorter, and G.D. Farquhar, *Aust. J. Plant Physiol.* **15**, 799 (1988).
- [23] A.G. Condon, R.A. Richards, and G.D. Farquhar, *Crop Sci.* **27**, 996 (1987).
- [24] G.H. Rau, R.E. Sweeny, I.R. Kaplan, A.J. Means, and D.R. Young, *Est. Coast. Shelf Science* **13**, 701 (1981).
- [25] C.D. Keeling, S.C. Piper, R.B. Bacastow, M. Wahlen, T.P. Worf, M. Heimann, and H.A. Meijer, SIO Reference Series, No. 01-06 (Scripps Institution of Oceanography, San Diego, 2001).
- [26] C.D. Keeling, S.C. Piper, R.B. Bacastow, M. Wahlen, T.P. Worf, M. Heimann, and H.A. Meijer, in *A History of Atmospheric CO₂ and its Effects on Plants, Animals, and Ecosystems*, edited by J.R. Ehleringer, T.E. Cerling, and M.D. Dearing (Springer Verlag, New York, 2005), pp. 83–111.
- [27] R.J. Francey, C.E. Allison, D.M. Etheridge, C. Trudinger, I. Enting, M. Luenberger, R. Langenfelds, E. Michel, and L. Steele, *Tellus* **51B**, 170 (1999).
- [28] H. Friedli, H. Lottschner, H. Oeschger, U. Siegenthaler, and B. Stauffer, *Nature* **324**, 237 (1986).
- [29] W.G. Cochran, *Biometrics* **13**, 261 (1957).
- [30] K.T. Hubick, G.D. Farquhar, and R. Shorter, *Aust. J. Plant Physiol.* **13**, 803 (1986).
- [31] S.S. Butcher, R.J. Charlson, G.H. Orians, and G.V. Wolfe, *Global Biogeochemical Cycles* (Academic Press, San Diego, 1992).
- [32] D. Schimel, D. Alves, I. Enting, M. Heimann, F. Joos, D. Raynaud, and T. Wigley, in *Climate Change 1994: Radiative Forcing of Climate Change and an Evaluation of the IPCC IS92 Emission Scenarios*, edited by J.T. Houghton, *et al.* (Cambridge University Press, New York, 1995), pp. 76–86.
- [33] T.J. Blasing, C.T. Broniak, and G. Marland, Carbon Dioxide Information Analysis Center, Oak Ridge National Laboratory, Oak Ridge, TN (2004).
- [34] P. Kohler, J. Schmitt, and H. Fischer, *Biogeosciences Discuss* **3**, 513 (2006).
- [35] R.A. Houghton, J.L. Hackler, and K.T. Lawrence, *Science* **285**, 574 (1999).
- [36] N. Gruber, C.D. Keeling, R.B. Bacastow, P.R. Guenther, T.J. Lueker, M. Wahlen, H.A.J. Meijer, W.G. Mook, and T.F. Stocker, *Global Biogeochemical Cycles* **13**, 307 (1999).
- [37] C.D. Keeling, R.B. Bacastow, A.F. Carter, S.C. Piper, T.P. Whorf, M. Heimann, W.G. Mook, and H. Roeloffzen, In: *Aspects of Climate Variability in the Pacific and Western Americas*. (ed. D. H. Peterson) pp. 165–236. Geophysical Mono 55 (American Geophysical Union, Washington D.C., 1989).
- [38] L.B. Flanagan and J.R. Ehleringer, *Tree* **13**, 10 (1998).
- [39] N. Nickerson and D. Risk, *Geophysical Research Letters* **36**, LO8401 (2009).
- [40] S.A. Carelton, B.O. Wolf, and C.M. del Rio, *Oecologia* **141**, 1 (2004).
- [41] J. Karlsson, *Oikos* **116**, 1691 (2007).
- [42] G.T. Marland, A. Boden, and R.J. Andres, Carbon Dioxide Information Analysis Center, Oaks Ridge National Laboratory, Oak Ridge, TN (2003).